THE JOURNAL OF PHYSICAL CHEMISTRY A LETTERS

2009, *113,* 8830–8833
Published on Web 07/10/2009

Alternate Cu_2 and Er_2 Spin Carriers in a Carboxylate-Bridged Chain: EPR Study

Rafael Calvo,*,† Raul E. Rapp,‡ Rosana P. Sartoris,† Ricardo C. Santana,§ and Mireille Perec*,∥

Departamento de Física, Facultad de Bioquímica y Ciencias Biológicas, Universidad Nacional del Litoral, and INTEC (CONICET-UNL), Güemes 3450, 3000 Santa Fe, Argentina, Instituto de Física, Universidade Federal do Rio de Janeiro, 21941-972, Rio de Janeiro, RJ, Brazil, Instituto de Física, Universidade Federal de Goiás, CP 131, 74001-970, Goiânia, GO, Brazil, and Departamento de Química Inorgánica, Analítica y Química Física, Facultad de Ciencias Exactas y Naturales, INQUIMAE, Universidad de Buenos Aires, Ciudad Universitaria, 1428 Buenos Aires, Argentina

Received: June 5, 2009; Revised Manuscript Received: July 2, 2009

We report powder EPR measurements at 9.48 GHz and temperatures of 4 K $\leq T \leq$ 300 K and at 33.86 GHz and T = 300 K for the polymeric compound $\{[Cu_2Er_2(L)_{10}(H_2O)_4]\cdot 3H_2O\}_n$ (HL = *trans*-2-butenoic acid) having alternate Cu_2 and Er_2 dinuclear units bridged by carboxylates along a chain. Above 70 K, when the Er^{III} resonance is unobservable and uncoupled from the Cu^{II} ions, the spectrum arises from the excited triplet state of antiferromagnetic Cu_2 units, decreasing in intensity as T decreases, and disappearing when these units condensate into the singlet ground state. Fit of a model to the spectra at 9.48 and 33.86 GHz and 300 K gives $g_{Cu}^{\parallel} = 2.379$, $g_{Cu}^{\perp} = 2.065$, $D_{Cu} = -0.340$ cm^{-1}, and $E_{Cu} \sim 0$ for the g-factors and zero field splitting parameters. From the T dependence of the intensity of the spectrum above 70 K, we obtain $J_{Cu-Cu} = -336(11)$ cm^{-1} for the intradinuclear exchange interaction. Below 50 K, a spectrum attributed to Er_2 units appears, narrows, and resolves as T decreases, due to the increase of the spin−lattice relaxation time T_1. The spectrum at 4 K allows calculating g values $g_1 = 1.489$, $g_2 = 2.163$, and $g_3 = 5.587$ and zero field splitting parameters $D_{Er} = -0.237$ cm^{-1} and $E_{Er} = 0.020$ cm^{-1}. The results are discussed in terms of the properties of the Cu and Er ions, and the crystal structure of the compound.

Introduction

Since the works of Bencini et al.,[1,2] many efforts have been oriented to prepare and characterize materials containing simultaneously ions of the 3d and 4f groups. Part of the interest arises from the possibility of obtaining molecular magnets[3] with large magnetic moments and anisotropy arising from the rare earths, large exchange couplings between 3d and 4f ions, and a slow evolution of the magnetization.[4,5] There are only a few examples of using EPR to investigate these compounds,[6,7] probably because of the complexities of interpreting magnetically coupled systems, and the absence of appropriate single crystal samples.[8]

We recently reported[9] the preparation, structures, and magnetic and EPR measurements for three isostructural $[Cu_2Ln_2]_n$ 1-D polymers $\{[Cu_2Ln_2(L)_{10}(H_2O)_4]\cdot 3H_2O\}_n$ (HL = *trans*-2-butenoic acid and Ln = Gd, Er, Y) with alternate Cu_2 and Ln_2 dinuclear units bridged by carboxylate ligands. The magnetic data for $[Cu_2Y_2]_n$ in which the Cu_2 dinuclear units are isolated by diamagnetic Y_2 units indicated AFM coupling $J_{Cu-Cu} = -338(3)$ cm^{-1} between copper ions. The EPR spectrum of $[Cu_2Er_2]_n$ observed at 300 K was similar to that of the magnetically isolated Cu_2 dinuclear units in $[Cu_2Y_2]_n$.[9] A more detailed study was needed to characterize $[Cu_2Er_2]_n$, where Er^{III} is an open shell lanthanide, and in this direction, we report here EPR measurements for $[Cu_2Er_2]_n$ at two microwave frequencies, as a function of T. The observed strong variation of the spectra with T allows us to separate the contributions from Cu_2 and Er_2 units, and to evaluate their magnetic parameters by simulation of the spectra at high and low T, respectively. Our work explores the interesting possibilities offered by EPR to study complex magnetically coupled systems.

Experimental Methods and Results

$[Cu_2Er_2]_n$ was prepared as described, and the structural features are shown in Figure 1.[9] We used $MgO:Cr^{III}$ (g = 1.9797) and unintentional Fe^{III} impurities in the sample tube, as field and EPR signal intensity markers. EPR spectra of powdered samples were collected at temperatures between 4 and 300 K with Bruker spectrometers ESP 300, working at 33.86 GHz, and Elexsys E580, working at 9.48 GHz, respectively, and analyzed with EasySpin.[10] Figure 2 displays the spectra $[d(\chi)''/dB_0]$ of a powdered sample of $[Cu_2Er_2]_n$ observed at 9.48 GHz at 4 K < T < 300 K. Figure 3 displays the spectra observed at 300 K and 33.86 GHz (a) and 9.48 GHz (b) and the spectrum at 9.48 GHz and T = 4 K (c), respectively. The spectra for $T >$ 70 K in Figure 2 are similar to that observed[9] at 300 K for $[Cu_2Y_2]_n$. The peaks around 30 mT (strong), 468 mT (strong), and 600 mT (weak), labeled as B_{z_1}, $B_{x_2y_2}$, and B_{z_2} in Figure 2, arising from the S = 1 excited triplet state of the Cu_2 dinuclear units, have been observed in similar dinuclear Cu^{II} compounds.[11,12]

* To whom correspondence should be addressed. E-mail: calvo@fbcb.unl.edu.ar (R.C.); perec@qi.fcen.uba.ar (M.P.).
† Universidad Nacional del Litoral and INTEC (CONICET-UNL).
‡ Universidade Federal do Rio de Janeiro.
§ Universidade Federal de Goiás.
∥ Universidad de Buenos Aires.

10.1021/jp905310t CCC: $40.75

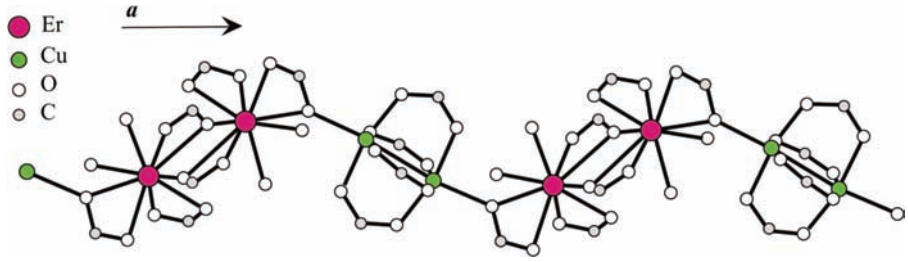

Figure 1. Structure of the $[Cu_2Er_2]_n$ chain as reported in ref 6. Only the relevant atoms are shown.

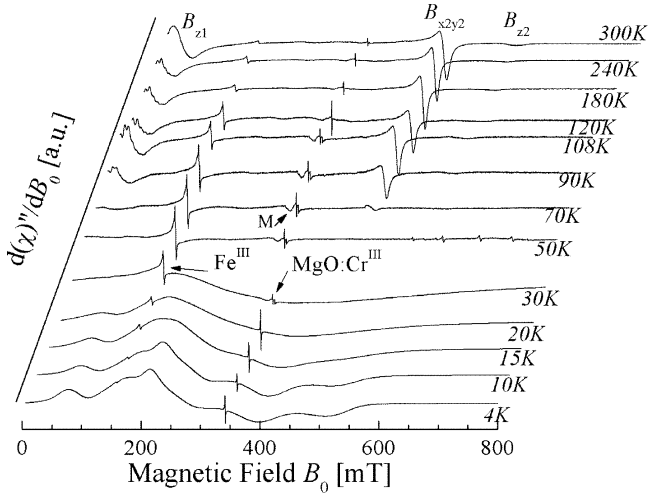

Figure 2. Temperature variation of the EPR spectra of a powder sample of $[Cu_2Er_2]_n$. All spectra are normalized to present the same peak-to-peak span.

Their intensities decrease with decreasing temperature as a consequence of the condensation of the AFM Cu dinuclear units in the $S = 0$ nonmagnetic ground state. The peak M at $B_0 =$ 325 mT whose intensity increases with decreasing temperature as for a paramagnet[13] is assigned to monomeric Cu^{II} impurities present in the sample. The peaks at ~340 and ~160 mT arise from $MgO:Cr^{III}$ and Fe^{III}, respectively. Figure 3a also shows the forbidden $\Delta M = \pm 2$ double quantum transition at 511 mT, the peak $B_{x_1y_1}$ at 982 mT, and the peaks B_{z_2} and $B_{x_2y_2}$ that are superimposed at 1332 mT. The peak B_{z_1} at 30 mT in Figure 2 displays hyperfine structure with seven components, arising from the coupling with the two copper nuclei in the Cu_2 unit for $T <$ 240 K. The T dependence of this structure indicates narrowing and higher resolution at lower temperatures, when the Cu_2 units condensate to the nonmagnetic singlet state, and the dipole−dipole interactions decrease.[14−16] At low T, the signal attributed to the Cu_2 units disappears, and the contribution from the Er_2 units becomes stronger (Figures 2 and 3c) when the spin−lattice relaxation of the Er ions slows down.

Analysis of the Data

Cu_2 Dinuclear Units. The EPR spectra of $[Cu_2Er_2]_n$ at 300 K (Figures 2 and 3a,b) are described by the spin Hamiltonian:[9]

$$\mathscr{H}_{Cu} = \mu_B \mathbf{B}_0 \cdot \mathbf{g}_{Cu} \cdot (\mathbf{S}_{Cu_1} + \mathbf{S}_{Cu_2}) - J_{Cu-Cu} \mathbf{S}_{Cu_1} \cdot \mathbf{S}_{Cu_2} + \mathbf{S}_{Cu_1} \cdot \mathbf{D}_{Cu} \cdot \mathbf{S}_{Cu_2} \quad (1)$$

where $\mathbf{S}_{Cu_1}$ and $\mathbf{S}_{Cu_2}$ are spin $^1/_2$ operators corresponding to the copper ions in a unit, $\mathbf{g}_{Cu}$ is the axial g-matrix, J_{Cu-Cu} is the isotropic (Heisenberg) exchange coupling responsible for the energy splitting between singlet and triplet states, and $\mathbf{D}_{Cu}$ is

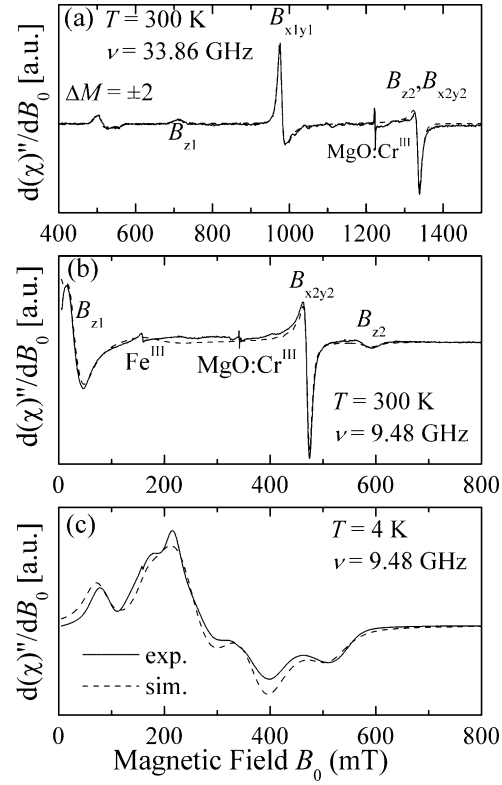

Figure 3. EPR spectra of a powder sample of $[Cu_2Er_2]_n$ at 300 K: (a) 33.86 GHz, 300 K; (b) 9.48 GHz, 300 K; (c) 9.48 GHz, 4 K. Solid lines are the experimental results; dashed lines are simulations using the parameters given in the text.

the symmetric matrix considering the dipole−dipole and anisotropic exchange contributions to the zero field splitting. We used Easyspin[10] to fit eq 1 to the spectra at 300 K in Figure 3a,b. Assuming that $\mathbf{g}_{Cu}$ and $\mathbf{D}_{Cu}$ have the same principal axes, we calculated $g_{Cu}^{\parallel} = 2.379(2)$ and $g_{Cu}^{\perp} = 2.065(2)$ for the principal g-factors and $D_{Cu} = -0.340(3)$ cm^{-1} and $E_{Cu} \sim 0$ for the zero field splitting parameters. The spectra simulated with these values are in good agreement with the experiment. The parameters obtained are essentially equal to those for the isostructural compound $[Cu_2Y_2]_n$ where Y is a diamagnetic ion,[9] and to those for related compounds.[14] In eq 1, we neglect the coupling of the copper spins with those of the Er^{III} ions. This is possible at high temperatures when the spin−lattice relaxation of Er^{III} is so fast that the Cu−Er interaction is time averaged to zero because the Cu ions cannot follow the fast dynamics of the Er^{III} ions. The coupling between Cu and Er ions can be ignored in eq 1 when the Er relaxation rates are larger than the zero field splitting of the Cu_2 units.[8] As most rare earth ions with orbital degeneracy, Er^{III} ions have large spin−lattice relaxation rates ($1/T_1$) because the lattice vibrations strongly interact with the magnetic ion and the number of phonons with energies similar to the crystal field splitting (Δ) is very large.[17]

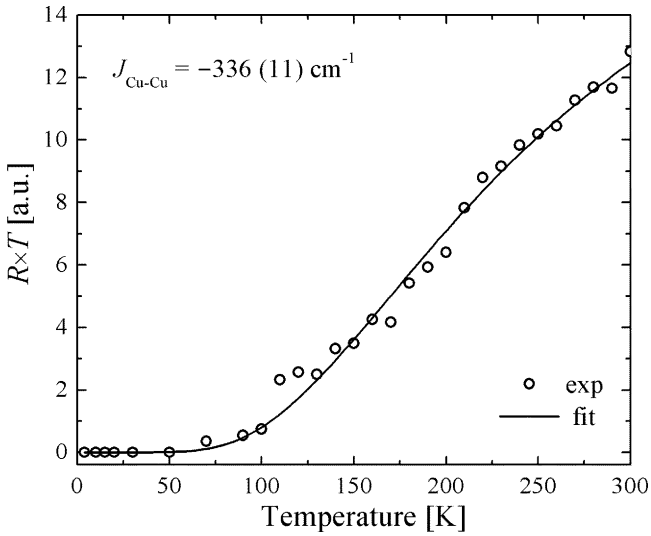

Figure 4. Temperature variation of the ratio R between the integrated areas of the signals $B_{x_2y_2}$ corresponding to the Cu_2 unit and that of the Cr^{III} marker, multiplied by T. The solid line is the best fit of eq 2.

The Orbach relaxation process, $1/T_1 \propto \Delta^3 \exp(-\Delta/k_BT)$, may change $1/T_1$ several orders of magnitude for a temperature change of a few degrees.[17]

We calculate the exchange interaction J_{Cu-Cu} for $[Cu_2Er_2]_n$ from the T variation between 300 and 50 K of the ratio $R(T)$ between the integrated areas of the signals $B_{x_2y_2}$ of the Cu_2 unit and that of the Cr^{III} marker with a procedure avoiding changes with T of the experimental setup.[13,16] The product $T \times R(T)$ as a function of T in Figure 4 allows calculating J_{Cu-Cu} in $[Cu_2Er_2]_n$ using the Bleaney−Bowers equation:[18]

$$T \times R(T) \propto \frac{2}{3 + \exp(-J_{Cu-Cu}/k_BT)} \quad (2)$$

Fitting eq 2 to the data in Figure 4, we obtained $J_{Cu-Cu} = -336(11)$ cm^{-1} (with a statistical coefficient of determination of $R^2 = 0.9918$) for the AFM exchange coupling parameter within the Cu_2 unit, that compares well with that observed in the similar compounds $[Cu_2Y_2]_n$ and $Cu_2(L)_4(DMF)_2$.[9,14] We emphasize that it would not be possible to obtain J_{Cu-Cu} from magnetic measurements because the contributions to the susceptibility and magnetization of the Cu_2 units in $[Cu_2Er_2]_n$ are dominated by those of the Er_2 units.

Er_2 Dinuclear Units. The spectrum that narrows and grows with decreasing temperature below 50 K arises from the Er_2 dinuclear units. Er^{III} has a $(4f^{11})$ $^4I_{15/2}$ ground state multiplet, which splits into eight Kramers doublets by the crystal field. Only the ground doublet state is populated at 4 K, giving rise to the observed spectrum that may be described by

$$\mathcal{H}_{Er_2} = \mu_B \mathbf{B}_0 \cdot \mathbf{g}_{Er} \cdot (\mathbf{S}_{Er_1} + \mathbf{S}_{Er_2}) - J_{Er-Er} \mathbf{S}_{Er_1} \cdot \mathbf{S}_{Er_2} + \mathbf{S}_{Er_1} \cdot \mathbf{D}_{Er} \cdot \mathbf{S}_{Er_2} \quad (3)$$

with the approximation of equal principal axes for the matrices $\mathbf{g}_{Er}$ and $\mathbf{D}_{Er}$. Equation 3 neglects the contribution of the Cu spins to the behavior of the Er ions because at 4 K the Cu_2 dinuclear units condensate in the nonmagnetic ground singlet state. In addition, our analysis of the spectrum at 4 K neglects the small exchange interaction J_{Er-Er} ($|J_{Er-Er}|/k_B < 1$ K) with a singlet−triplet splitting with no effect on the spectrum. Fitting the Er_2 spectrum involves five parameters, plus those related to line broadening. We obtain the principal g values $g_1 = 1.489(3)$, $g_2 = 2.163(1)$, and $g_3 = 5.587(3)$, with strong orthorhombic anisotropy, and zero field splitting $D_{Er} = -0.237$ cm^{-1} and $E_{Er} = 0.020$ cm^{-1}. The spectrum simulated with these parameters (Figure 3c) is in reasonable agreement with the experimental result. The g-matrix of Er^{III} is expected to be strongly dependent on the crystal field at its site and displays large anisotropies.[19,20] With the information at hand, it is not possible to model their values. The hyperfine structure arising from the 22.9% abundant ^{167}Er isotope having $I = {}^7/_2$ would give 15 anisotropic peaks for an Er_2 unit, which seem to be lost in the powder spectrum, but are responsible for the small disagreement between experimental and calculated curves in Figure 3c.[19,20] For Er^{III} ions, the exchange couplings (isotropic and anisotropic) are small, and the zero field splitting is a consequence of dipole−dipole interactions between two Er^{III} ions at 4.21 Å in the dinuclear unit. Though the large anisotropy of the g-factor renders the calculation inaccurate, this value of D_{Er} is in qualitative agreement with a point dipole interaction.

Conclusions

The EPR spectrum of powder samples of $[Cu_2Er_2]_n$ shows a strong temperature dependence. Above 50 K, it arises essentially from the Cu_2 dinuclear units and the contribution of Er_2 dinuclear units is negligible due to the fast spin−lattice relaxation of the Er ions. Below 50 K, the Cu_2 units are mostly in the ground nonmagnetic singlet state, and the spectrum is totally due to the Er_2 dinuclear units. The temperature dependent EPR studies allowed separating the EPR spectra arising from Cu_2 and from Er_2 dinuclear units, and calculating the relevant magnetic parameters for each one. At high T, the Cu−Er interaction is averaged out by fast relaxation of the Er ions, isolating the Cu_2 units. The condensation of the Cu_2 units in the ground singlet state isolates magnetically the Er_2 units at low T, allowing their EPR spectrum to be modeled.

Acknowledgment. The work in Argentina was supported by grants of CONICET, PIP 5274, CAI+D-UNL, and ANPCyT PICT 25409. The work in Brazil was supported by CNPq, FAPERJ, and CAPES. The authors acknowledge Dr. A. J. Costa-Filho (IFSC, USP) for allowing us to use his Bruker ELEXSYS E-580 spectrometer. R.C. and M.P. are members of CONICET.

References and Notes

(1) Bencini, A.; Benelli, C.; Caneschi, A.; Carlin, R. L.; Dei, A.; Gatteschi, D. *J. Am. Chem. Soc.* **1985**, *107*, 8128–8136.
(2) Bencini, A.; Benelli, C.; Caneschi, A.; Dei, A.; Gatteschi, D. *Inorg. Chem.* **1986**, *25*, 572–575.
(3) Kahn, O. *Molecular Magnetism*; VCH: New York, 1993.
(4) Winpenny, R. E. P. *Chem. Soc. Rev.* **1998**, *27*, 447–452.
(5) Andruh, M.; Costes, J.-P.; Diaz, C.; Gao, S. *Inorg. Chem.* **2009**, *48*, 3342–3359.
(6) Caneschi, A.; Sorace, L.; Casellato, U.; Tomasin, P.; Vigato, P. A. *Eur. J. Inorg. Chem.* **2004**, 3887–3900.
(7) Tangoulis, V.; Costes, J.-P. *Chem. Phys.* **2007**, *334*, 77–84.
(8) Calvo, R. *Appl. Magn. Reson.* **2007**, *31*, 271–299.
(9) Calvo, R.; Rapp, R. E.; Chagas, E.; Sartoris, R. P.; Baggio, R.; Garland, M. T.; Perec, M. *Inorg. Chem.* **2008**, *47*, 10389–10397. The crystallographic information file (cif) containing the reported structural data for $[Cu_2Er_2]_n$ may be obtained from the Cambridge Crystallographic Data Centre (CCDC) as supporting information under number 687242, http://www.ccdc.cam.ac.uk/cgi-bin/catreq.cgi.
(10) Stoll, S. *Int. EPR Soc. Newsletter* **2003**, *13*, 24–26. Stoll, S.; Schweiger, A. *J. Magn. Reson.* **2006**, *178*, 42–55.
(11) Atherton, N. M. *Principles of Electron Spin Resonance*; Ellis Horwood: Chichester/Prentice-Hall: New York, 1993.

(12) Weil, J. A.; Bolton, J. R.; Wertz, J. E. *Electron Paramagnetic Resonance: Elementary Theory and Practical Applications*; Wiley: New York, 1994.

(13) Wasson, J. R.; Shyr, C. I.; Trapp, C. *Inorg. Chem.* **1968**, *7*, 469–473.

(14) Schlam, R.; Perec, M.; Calvo, R.; Lezama, L.; Insausti, M.; Rojo, T.; Foxman, B. M. *Inorg. Chim. Acta* **2000**, *310*, 81–88.

(15) Sebastian, S. E.; Tanedo, P.; Goddar, P. A.; Lee, S.-C.; Wilson, A.; Kim, S.; Cox, S.; McDonald, R. D.; Hill, S.; Harrison, N.; Batista, C. D.; Fisher, I. R. *Phys. Rev. B* **2006**, *74*, 180401.

(16) Napolitano, L. M. B.; Nascimento, O. R.; Cabaleiro, S.; Castro, J.; Calvo, R. *Phys. Rev B* **2008**, *77*, 214423.

(17) Finn, C. B.; Orbach, R.; Wolf, W. P. *Proc. Phys. Soc., London* **1961**, *77*, 261–268. Orbach, R. *Proc. R. Soc. London* **1961**, *A264*, 458–484, 485−495.

(18) Bleaney, B.; Bowers, K. D. *Proc. R. Soc. London* **1952**, *214*, 451–465.

(19) Abragam, A.; Bleaney, B. *Electron Paramagnetic Resonance of Transition Ions*; Clarendon Press: Oxford, U.K., 1970.

(20) Guillot-Noël, O.; Goldner, P. H.; Le Du, Y.; Baldit, E.; Monnier, P.; Bencheikh, K. *Phys. Rev. B* **2006**, *74*, 214409.

JP905310T